Preparation of the Solid Electrolytes $Li_{4+x}Al_xSi_{1-x}O_4$-yAl_2O_3 by the Sol-Gel Method and Study of Their Ionic Conductivity

CHEN, Ru-Fen* (陈汝芬) SONG, Xiu-Qin(宋秀芹)
Department of Chemistry, Hebei Normal University, Shijiazhuang, Hebei 050016, China

The $Li_{4+x}Al_xSi_{1-x}O_4$-yAl_2O_3 ($x = 0$ to 0.5, $y = 0$ to 0.5) ion conductors were prepared by the Sol-Gel method and examined in detail. The powder and sintered samples were characterized by TG-DTA, XRD, SEM, and AC impedance techniques. The experimental results show that the conductivity and sinterability increase with the amount of excess Al_2O_3 in the silicate. The particle size of the powder samples is about 0.13 μm. The maximum conductivity at 18 ℃ is 3.057×10^{-5} s/cm for $Li_{4.4}Al_{0.4}Si_{0.6}O_4$-0.3 Al_2O_3.

Keywords $Li_{4+x}Al_xSi_{1-x}O_4$-yAl_2O_3, solid electrolyte, ionic conductivity, Sol-Gel method

Introduction

Lithium ion conductors are promising materials for many kinds of electrochemical application, such as electrolytes for high-energy density batteries.[1] The properties of high ionic conductivity, high decomposition potential, stability and compatibility against electrodes should be satisfied when they are applied to solid electrolytes.

It is well known that Li_4SiO_4-based solid solutions increase greatly in conductivity when Si^{4+} is substituted by trivalent Al^{3+}.[2-8] The conductivity could be considerably increased by the mixing of binders such as Al_2O_3 phase. The reasons for the conductivity improvement have been ascribed to increased sinterability of the sintered pellet.[9-10]

In this paper, the $Li_{4+x}Al_xSi_{1-x}O_4$-yAl_2O_3 ($x = 0$ to 0.5, $y = 0$ to 0.5) composite solid electrolyte systems were prepared by the Sol-Gel method. The structure, ionic conductivity and sinterability were investigated.

Experimental

Synthesis of $Li_{4+x}Al_xSi_{1-x}O_4$-yAl_2O_3 by the Sol-Gel method

The $Li_{4+x}Al_xSi_{1-x}O_4$-yAl_2O_3 ($x = 0$ to 0.5, $y = 0$ to 0.5) were prepared by the Sol-Gel method using reagent grade Li_2CO_3, $Al(NO_3)_3$, $Si(OC_2H_5)_4$, HNO_3 and $NH_3 \cdot H_2O$. The C_2H_5OH was used as solvent for these materials having pH = 6. The solution was refluxed for 5 h at 85 ℃ and aged at 70 ℃ for gelation. The gels were vacuum dried and heated for several hours. The ultrafine powder at 650 ℃ was pressed into pellets, and then the sintered pellets were abstained at 700 ℃ for 5 h.

Measurements

The $Li_{4+x}Al_xSi_{1-x}O_4$-yAl_2O_3 ($x = 0$ to 0.5, $y = 0$ to 0.5) powder were characterized by X-ray diffraction patterns, recorded on a Rigaku/Rotaflex/RINT rotating anode diffractometer using Cu K_α radiation. Thermogravimetric (TG) and Differential Thermal Analysis (DTA) experiments were performed using a Rigaku-TG8101D thermal analyzer at a scan rate of 10 ℃/min. The shape and size of powder samples were examined using a scanning electron microscopy (SEM). The ionic conductivity measurements were carried out on the sintered samples in the form of pellets, which were polished and painted with Ag past on opposite faces. The AC

* E-mail: chenrf6@263.net
Received May 8,2001; revised July 27, 200; accepted August 27, 2001.
Project supported by the Natural Science Foundation of Hebei Province (No. 296169).

impedance of the samples was measured using an ac impedance system (EG&G, Princeton Applied Research, Model 378) that included a potentiostat/galvanostat (Model 273), a lock-in amplifier (Model 5208), and an IBM PS/2 computer. The frequency ranged from 5 Hz to 100 kHz. The characterized impedance spectra were simulated with the Equivalent Circuits program developed by Boukamp.[11]

Results and discussion

Thermal behavior

Fig. 1 shows the decompose process of the $Li_{4.4}Al_{0.4}Si_{0.6}O_4$-$0.3Al_2O_3$ gel, which occurs in four steps. The endothermic regions at 100—150 ℃, 200—300 ℃ and 400—620 ℃ are attributed to the water volatilization, the NO_3^- decomposition and the reaction of 2HO—Si≡ → ≡O—Si—O≡ + H_2O.[12] The small peak at 620—650 ℃ is due to the formation of $Li_{4.4}Al_{0.4}Si_{0.6}O_4$ solid solution. There are no any exothermic and endothermic peaks at high temperatures (> 650 ℃). The TG curve shows the weight loss of the sample. From the TG-DTA curves, the gel heat-treated temperatures are estimated to be 100—650 ℃. Other gel samples presented similar thermal behavior. The X-ray powder diffraction analysis also indicated the crystallization completed at 650 ℃.

Structure characterization

Fig. 2 shows the X-ray diffraction (XRD) patterns of $Li_{4.4}Al_{0.4}Si_{0.6}O_4$-$yAl_2O_3$ (a: $y = 0$; b: $y = 0.3$), which have been heated at 650 ℃ for 8 h. The result of XRD analysis shows that single phase solid solutions $Li_{4+x}Al_xSi_{1-x}O_4$ ($0 \leqslant x \leqslant 0.4$)) have been prepared at 650 ℃, which is much lower compared with synthesis temperature in solid state reaction (1100 ℃).[13] θ-Al_2O_3 phase is appeared for $y = 0.3$ in Fig. 2b. The solid solutions are isostructural with the monoclinic Li_4SiO_4. The reflection peaks in the powder diffraction pattern are indexed completely based on a monoclinic symmetry, $P2_1/m$ space group. The variation of the unit-cell parameters with x in the solid solution phases is shown in Table 1.

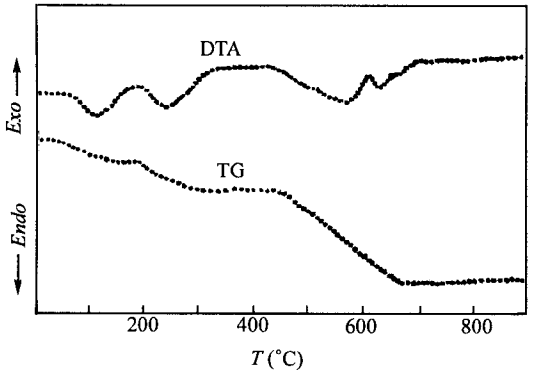

Fig. 1 TG-DTA curve of $Li_{4.4}Al_{0.4}Si_{0.6}O_4$-$0.3Al_2O_3$ gel.

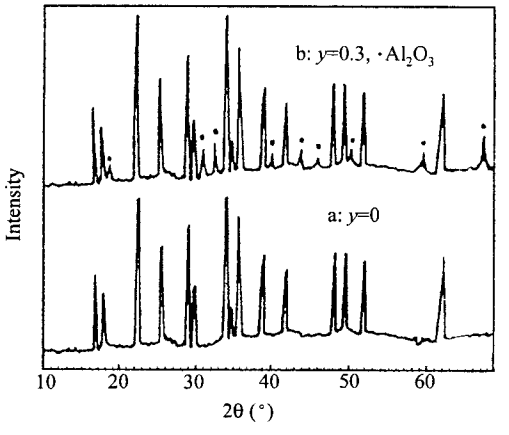

Fig. 2 XRD pattern of $Li_{4.4}Al_{0.4}Si_{0.6}O_4$-$yAl_2O_3$. a: $y = 0$; b: $y = 0.3$.

Table 1 Unit-cell parameters of $Li_{4+x}Al_xSi_{1-x}O_4$ compositions

	x	a (nm)	b (nm)	c (nm)	β (°)	V (nm^3)
Li_4SiO_4	0	0.52972	0.61019	0.51487	90.25	0.16642
$Li_{4+x}Al_xSi_{1-x}O_4$	0.1	0.53051	0.61099	0.51592	90.22	0.16723
	0.2	0.53038	0.61301	0.51709	90.22	0.16812
	0.3	0.53049	0.61502	0.51845	90.21	0.16915
	0.4	0.53066	0.61663	0.51959	90.20	0.17002

The lattice parameters increase with increasing x because of the larger ionic radius Al^{3+} compared with that of Si^{4+} for $Li_{4+x}Al_xSi_{1-x}O_4$ ($0 \leqslant x \leqslant 0.4$) systems. These results are completely consistent with the results of Christian Masquelier, who prepared $Li_{4+x}Al_xSi_{1-x}O_4$ by the solid state reaction.[7] Fig. 3 shows the scanning electron microscopy picture of the powder samples for $Li_{4.4}Al_{0.4}Si_{0.6}O_4$-$0.3Al_2O_3$. From this picture it can be found that the shape of samples is spherical and their average diameter is about 0.13 μm.

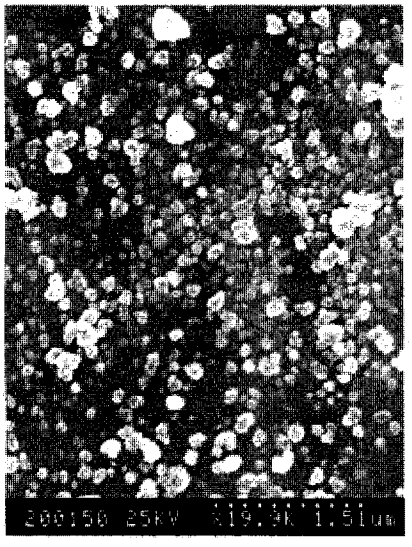

Fig. 3 SEM picture of $Li_{4.4}Al_{0.4}Si_{0.6}O_4$-$0.3Al_2O_3$.

Ionic conductivity

The relation between the porosity of the sintered pellets and the y value for $Li_{4.4}Al_{0.4}Si_{0.6}O_4$-$yAl_2O_3$ is shown in Fig. 4. As can be seen, the porosity tends to have low values with the enhancement of Al_2O_3. Other samples have similar density.

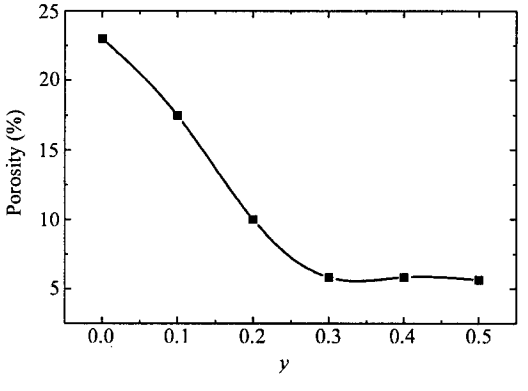

Fig. 4 Variation of the porosity for $Li_{4.4}Al_{0.4}Si_{0.6}O_4$-$yAl_2O_3$.

The impedance spectra from the electrochemical cell $Ag/Li_{4+x}Al_xSi_{1-x}O_4$-$yAl_2O_3/Ag$ are interpreted in terms of bulk, grain boundary and Warbarg impedance. Typical complex impedance diagram for the $Li_{4.4}Al_{0.4}Si_{0.6}O_4$-$0.3Al_2O_3$ measured at 18 ℃ is shown in Fig. 5. Similar electric behavior has been observed for all the other samples. In Fig. 5, the semicircle in the higher frequency region is attributed to the bulk of grain, while the spike in the low frequency is attributed to the grain boundary.[14] The bulk, grain boundary and total ionic conductivity for $Li_{4+x}Al_xSi_{1-x}O_4$-yAl_2O_3 are obtained from $\sigma = d/R \cdot S$, where d and S are the thickness and sectional area of the pellet, respectively.

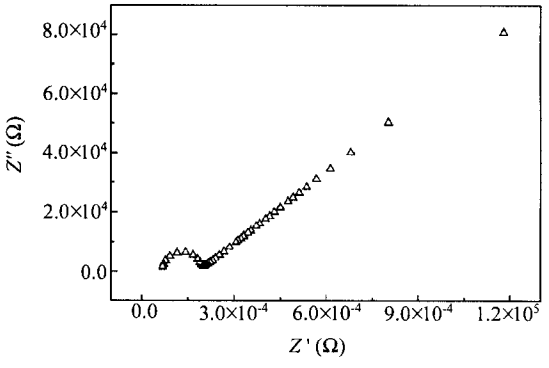

Fig. 5 Complex impedance of $Li_{4.4}Al_{0.4}Si_{0.6}O_4$-$0.3\ Al_2O_3$.

Fig. 6 presents the conductivity (at 18 ℃) dependence on x for $Li_{4+x}Al_xSi_{1-x}O_4$. The conductivity is seen to be enhanced by the Al^{3+} substitution and maximum conductivity is obtained at $x = 0.4$.

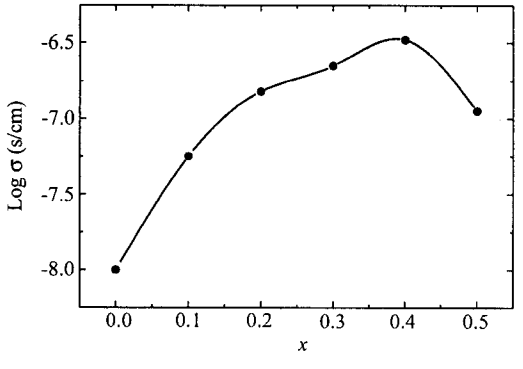

Fig. 6 Variation of the logσ at 18 ℃ on x for $Li_{4+x}Al_xSi_{1-x}O_4$.

The ionic bulk σ_1, grain boundary σ_2 and total σ conductivity for $Li_{4.4}Al_{0.4}Si_{0.6}O_4$-$yAl_2O_3$ systems at

18 ℃ are shown in Table 2.

Table 2 Conductivity of bulk σ_1, grain boundary σ_2 and total σ for $Li_{4.4}Al_{0.4}Si_{0.6}O_4$-$yAl_2O_3$

yAl_2O_3	0.00	0.10	0.20	0.30	0.40	0.50
σ_1 ($\times 10^{-5}$)	4.998	5.236	5.881	5.879	5.642	5.527
σ_2 ($\times 10^{-6}$)	2.434	9.749	24.87	63.69	20.96	10.15
σ_2 ($\times 10^{-6}$)	2.321	9.545	17.48	30.57	15.29	8.576

It is seen from Table 2 that the grain boundary ionic conductivity increases with the amount of excess Al_2O_3, while bulk conductivity almost has no change. It is because the structure of samples has not been changed with increasing Al_2O_3. Addition of the second phase Al_2O_3 results in the increase of the sintered pellet density, which is very effective for the enhancement of the grain boundary conductivity. The lithium silicate is formed at the grain boundaries during the heating process, and then the surface of grains is melted and recrystallized at the flux. The second Al_2O_3 phase acts as a flux to accelerate the sintering process and to obtain high conductivity grain boundaries. However, the conductivity of samples decreases at $y > 0.3$. Probably the ion moving is obstructed with the increased greatly amount of Al_2O_3. The maximum conductivity is obtained at around $y = 0.3$ for all the systems examined. Further work is underway in our laboratory.

Conclusion

Solid electrolytes, which belong to $Li_{4+x}Al_xSi_{1-x}O_4$-yAl_2O_3 systems, were prepared by the Sol-Gel method. The synthetic temperature of powder samples is much lower compared with synthesis temperature in solid state reaction. The partial substitution of the Si^{4+} with Al^{3+} in the Li_4SiO_4 system was very effective for the enhancement of the conductivity. Mixing binders such as Al_2O_3 with $Li_{4+x}Al_xSi_{1-x}O_4$ are also successful in obtaining a high conductivity. The reasons for the conductivity improvement have been ascribed to increase sinterability of the sintered pellet. The maximum conductivity at 18 ℃ is 3.057×10^{-5} s/cm for $Li_{4.4}Al_{0.4}Si_{0.6}O_4$-$0.3Al_2O_3$.

References

1 Saito, Y.; Asai, T.; Ado, K.; Kageyama, H.; Nakamura, O. *Solid State Ionics* **1990**, *40/41*, 34.

2 Shannon, D.; Taylor, B. E.; English A. D.; Berzins, T. *Electrochim. Acta* **1977**, *22*, 783.

3 Jackowska, K.; West, A. R. *J. Mater. Sci.* **1983**, *18*, 2380.

4 Quintana, P.; West, A. R.; West, B. *Ceram. Trans.* **1989**, *88*, 17.

5 Quintana, P.; Velasco, F.; West, A. R. *Solid State Ionics* **1989**, *34*, 149.

6 Saito, Y.; Ado, K.; Asai, T.; Kageyama, H.; Nakamura, O. *Solid State Ionics* **1991**, *47*, 149.

7 Masquelier, C.; Tabuchi, M.; Takeuchi, T. *Solid State Ionics* **1995**, *79*, 98.

8 Chen, R. F.; Song, X. Q.; Liu, H. T. *Chin. J. Inorg. Chem.* **2000**, *16*(6), 959 (in Chinese).

9 Liang, C. C. *J. Electrochem. Soc.* **1973**, *120*, 1289.

10 Zhu, B.; Lai, Z. H.; Mellander, B. E. *Solid State Ionics* **1994**, *70/71*, 125.

11 Boukamp, B. A. *Equivalent Circuit Users Manua & Software* (*Ver.* 4.51), the Netherlands University of Twente, **1993**, p. 18.

12 Sun, G.; Yang, S.; Zhang, Z. D. *Huaxue Tongbao* **1990**, *11*, 45 (in Chinese).

13 Raistrick, I. D.; Chun, H.; Huggins, R. A. *J. Electrochem. Soc.* **1976**, *123*(10), 1469.

14 Guo, Z. K.; Yan, Y. M. *Chin. Silic. Soc.* **1986**, *14* (3), 319 (in Chinese).

(E0105082 LI, L. T.; LING, J.)